

## Tevatron measurement of single top quark cross sections and the CKM matrix element $|V_{tb}|$

The Tevatron Electroweak Working Group<sup>1</sup>  
for the CDF and DØ Collaborations

### Abstract

We present the final combinations of CDF and DØ measurements of the cross section for single-top-quark production in proton-antiproton collisions at a center-of-mass energy of 1.96 TeV. The data correspond to total integrated luminosities of up to  $9.7 \text{ fb}^{-1}$  per experiment. The  $t$ -channel cross section is measured to be  $\sigma_t = 2.25_{-0.31}^{+0.29}$  pb. We also present the simultaneously measured  $s$ - and  $t$ -channel cross sections and the  $s+t$  combined cross section measurement resulting in  $\sigma_{s+t} = 3.30_{-0.40}^{+0.52}$  pb, without assuming the SM ratio of  $\sigma_s/\sigma_t$ . The modulus of the CKM matrix element obtained from the  $s+t$ -channel measurement is  $|V_{tb}| = 1.02_{-0.05}^{+0.06}$  and its value is used to set a lower limit of  $|V_{tb}| > 0.92$  at 95% C.L.

---

<sup>1</sup>The Tevatron Electroweak Working Group can be contacted at [tev-ewwg@fnal.gov](mailto:tev-ewwg@fnal.gov).  
More information can be found at <http://teveewwg.fnal.gov>.

# 1 Introduction

The top quark is the heaviest and one of the most puzzling elementary particles of the standard model (SM). Detailed studies of top quark production and decay provide powerful tests of strong and electroweak interactions, as well as sensitivity to physics beyond the standard model (BSM) [1]. At the Tevatron, protons ( $p$ ) and antiprotons ( $\bar{p}$ ) are collided at a center-of-mass energy of  $\sqrt{s} = 1.96$  TeV. Top quarks are produced predominantly in pairs ( $t\bar{t}$ ) via the strong interaction [2]. They are also produced singly via the electroweak interaction. The cross section for single-top-quark production depends strongly on the square of the magnitude of the quark-mixing Cabibbo-Kobayashi-Maskawa matrix [3] element  $V_{tb}$ , and consequently is sensitive to contributions from a fourth generation of quarks [4, 5], as well as other new phenomena [6].

In  $p\bar{p}$  scattering, single-top-quark production proceeds via the exchange of a virtual  $W$  boson that interacts with a  $b$  quark in the  $t$  channel [7, 8, 9], via the exchange of an intermediate  $W$  boson in the  $s$  channel [10], or in association with a  $W$  boson ( $Wt$ ) [11]. The predicted SM cross section for the  $t$ -channel process is  $2.10 \pm 0.13$  pb [9] while the  $s$ -channel cross section is  $1.05 \pm 0.06$  pb [12] for a top quark mass of 172.5 GeV. The cross section for  $Wt$  production is negligibly small at the Tevatron and therefore not considered in this note. Since the magnitude of the  $Wtb$  coupling is much larger than that of  $Wtd$  or of  $Wts$  [13], each top quark decays almost exclusively to a  $W$  boson and a  $b$  quark.

Observation of single-top-quark production, in all channels combined, was reported by the CDF [14, 15, 16] and D0 [17, 18] collaborations. The CDF collaboration subsequently measured a single-top-quark production cross section for the combined  $s$ ,  $t$ , and  $Wt$  channels of  $\sigma_{s+t+Wt} = 3.04_{-0.53}^{+0.57}$  pb using  $7.5 \text{ fb}^{-1}$  [19] and of the combined  $s$  and  $t$  channels  $\sigma_{s+t} = 3.02_{-0.48}^{+0.49}$  pb using data with up to  $9.5 \text{ fb}^{-1}$  of integrated luminosity [20]. The D0 collaboration obtained  $\sigma_{s+t} = 4.11_{-0.55}^{+0.60}$  pb for the combined  $s$  and  $t$  channels using  $9.7 \text{ fb}^{-1}$  of data [21].

After establishing the  $s + t$  process, the cross sections for individual production modes were measured independently. The D0 collaboration observed the  $t$ -channel process [22], and measured its cross section to be  $\sigma_t = 3.07_{-0.49}^{+0.54}$  pb using  $9.7 \text{ fb}^{-1}$  of data [21]. The CDF collaboration measured  $\sigma_{t+Wt} = 1.66_{-0.47}^{+0.53}$  pb using  $7.5 \text{ fb}^{-1}$  of data [19] and  $\sigma_t = 1.65_{-0.36}^{+0.38}$  pb using data with up to  $9.5 \text{ fb}^{-1}$  [20]. The difference of the results on  $\sigma_t$  between the CDF and D0 collaborations is of the order of 2 standard deviations (S.D.).

Based on evidence from both collaborations [23, 24, 21], CDF and D0 combined their results to observe the  $s$ -channel process with a cross section  $\sigma_s = 1.29_{-0.24}^{+0.26}$  pb [25]. All measurements are in agreement with SM predictions [12, 9]. At the CERN LHC proton-proton ( $pp$ ) collider, the  $t$ -channel production was observed by the ATLAS and CMS collaborations [26, 27, 28, 29]. Furthermore, ATLAS has found evidence for  $Wt$  associated production [30] and CMS has recently reported observation of this process [31].

## 2 Measurement overview and selections

In this note, we report combinations of single-top-quark cross section measurements, in analyses performed by the CDF [20] and D0 [21] collaborations using up to  $9.7 \text{ fb}^{-1}$  of integrated luminosity per experiment. In particular, we present a combined  $t$ -channel cross section, combined simultaneous measurements of the  $t$ -channel and  $s$ -channel cross sections, and a combination of  $s + t$ -channel cross sections (leading to a higher precision than just adding up the single results for the measured  $s$ - and  $t$ -channel cross sections). Here we do not repeat the measurement of the  $s$ -channel cross section, which were reported in Ref. [25].

The CDF and D0 detectors are described in detail in Refs. [32, 33]. The data are selected using a logical OR of many online selection requirements that preserve high signal efficiency for offline analysis. Both collaborations analyzed events with a lepton ( $\ell = e$  or  $\mu$ ) plus jets and missing transverse momentum  $\cancel{E}_T$  sensitive to single-top-quark decays to a  $W$  boson with subsequent decay to  $\ell\nu$ . We select events that contain (i) only one isolated lepton  $\ell$  with large transverse momentum  $p_T$ , (ii) a large imbalance in transverse momentum  $\cancel{E}_T$ , (iii) two or three jets with large  $p_T$ , and (iv) one or two  $b$ -tagged jets. To identify  $b$  jets, multivariate techniques are used to discriminate  $b$  jets from jets originating from light quarks and gluons [34, 35]. Additional selection criteria are applied to exclude kinematic regions that are difficult to model, and to minimize the quantum chromodynamic (QCD) multijet background where one jet is misreconstructed as a lepton and spurious  $\cancel{E}_T$  arises from mismeasurements.

The other final-state topology, analyzed by the CDF collaboration, involves  $\cancel{E}_T$  and jets, but no reconstructed isolated charged leptons ( $\cancel{E}_T$ +jets). The CDF analysis avoids overlap with the  $\ell$ +jets sample by vetoing events with identified leptons [24]. Large  $\cancel{E}_T$  is required, and events with either two or three reconstructed jets are accepted. This additional sample increases the acceptance for signal events by encompassing those in which the  $W$ -boson decay produces a lepton that is either not reconstructed or not isolated, or a  $\tau$  lepton that decays into hadrons + neutrino, which are reconstructed as a third jet. After the basic event selections, QCD multijet events dominate the  $\cancel{E}_T$ +jets event sample. To reduce this multijet background, a neural-network event selection is optimized to preferentially select signal-like events.

Events passing the  $\ell$ +jets and  $\cancel{E}_T$ +jets selections are separated into independent analysis channels, based on the number of reconstructed jets as well as on the number and quality of  $b$ -tagged jets. Each of the analyzed channels has a different background composition and signal to background ratio, and analyzing them separately enhances the sensitivity to single-top-quark production by approximately 10% [20, 21].

Several differences in the properties of  $s$ - and  $t$ -channel events can be used to distinguish them from one another. Events originating from  $t$ -channel production typically contain one light-flavor jet at large  $|\eta|$ , which is useful for distinguishing them from events associated with  $s$ -channel production and other SM background processes. Events from the  $s$ -channel process are more likely to contain two  $b$  jets originating from  $b$  quarks within the central region of the

detector, where they can be identified. Hence, single-top-quark events with two identified  $b$  jets are more likely to originate from  $s$ -channel production.

### 3 Modeling of signal and backgrounds

Both collaborations use Monte Carlo (MC) generators to simulate kinematic properties of signal and background events, except in the case of multijet production, which is modeled based on data. The CDF analysis models single-top-quark signal events at next-to-leading-order (NLO) accuracy in the strong coupling strength  $\alpha_s$  using the POWHEG [36] generator. The D0 analysis uses the SINGLETOP [37] event generator, based on NLO COMPHEP calculations that match the kinematic features predicted by other NLO calculations [38, 39]. Spin information in the decays of the top quark and the  $W$  boson is preserved in both POWHEG and SINGLETOP.

Kinematic properties of background events associated with the  $W$ +jets and  $Z$ +jets processes are simulated using the ALPGEN leading-order MC generator [40], and those for diboson contributions ( $WW$ ,  $WZ$  and  $ZZ$ ) are modeled using PYTHIA [41]. The  $t\bar{t}$  process is modeled using PYTHIA in the CDF analysis and by ALPGEN in the D0 analysis. The mass of the top quark in simulated events is set to  $m_t = 172.5$  GeV, which is consistent with the current world average value [42]. Higgs-boson processes are modeled using simulated events generated with PYTHIA for a Higgs mass of  $m_H = 125$  GeV [43, 44, 45]. In all of the above cases, PYTHIA is used to model proton remnants and to simulate the hadronization of all generated partons. The presence of additional  $p\bar{p}$  interactions is modeled by overlaying events selected from random beam crossings matching the instantaneous luminosity profile in the data. All MC events are processed through GEANT-based detector simulations [46], and reconstructed using the same software packages as used for collider data.

Predictions for the normalization of simulated contributions from background processes are estimated using both simulation and data. Data are used to normalize  $W$ -boson production associated with both light- and heavy-flavor jet contributions using enriched  $W$ +jets data samples that have negligible signal content [21, 16, 24]. All other simulated background samples are normalized to their theoretical cross sections, i.e. for  $t\bar{t}$  at next-to-NLO [47], for  $Z$ +jets and diboson production at NLO [48], and for Higgs-boson production including all relevant higher-order QCD and electroweak corrections [49]. For the measurement of the  $t$ -channel single-top-quark production cross section, the  $s$ -channel single-top-quark background sample is normalized to the NLO cross section combined with next-to-next-to-leading log (NNLL) resummations [12].

Differences observed between simulated events and data in lepton- and jet-reconstruction efficiencies, resolutions, jet-energy scale (JES), and  $b$ -tagging efficiencies are adjusted in the simulation to match observations in data, through correction functions obtained from measurements in independent data samples.

## 4 Combination method

Since there is no single kinematic variable that provides sufficient isolation of the single-top-quark signal from the dominant backgrounds, multivariate discriminants are optimized to separate signal events in each of the analyses from large background contributions. We utilize the  $s$ - and  $t$ -channel discriminants from CDF [23] and D0 [21] single top quark measurements. We form a binned likelihood as a product of all analysis channels from both collaborations in the bins of these multivariate discriminants, comparing data to the predictions for each contributing signal and background process. Using a Bayesian statistical analysis [50], we then derive combined Tevatron cross section measurements, taking the prior density for the signal cross sections to be uniform for non-negative cross sections.

## 5 Systematic uncertainties

The sources of uncertainties considered are identical to those used in Ref. [25], where more details can be found. We consider systematic uncertainties on the integrated luminosity from detector-specific sources and from the inelastic and diffractive cross sections, on the signal modeling, on the simulation of background, on data-based methods to estimate background, on detector modeling, on  $b$ -jet tagging and on the measurement of JES. The categories that contribute uncertainties in the distribution of the output of the final multivariate discriminant, and the values for the range of uncertainties applied to the predicted normalizations for signal and background contributions in each category of uncertainty are given in Table 1 of Ref. [25]. Reference [25] also gives the sources of systematic uncertainty common to measurements of both collaborations that are assumed to be 100% correlated, and which uncertainties are assumed to be uncorrelated. The dependence of the results on these correlations is negligible.

A two-dimensional (2D) posterior probability density is constructed as a function of  $\sigma_s$  and  $\sigma_t$  in analogy to the 1D posterior probability described in Ref. [25]. The measured cross section is quoted as the value at the position of the maximum, and the area of the distribution in the most narrow region that encompasses 68% of the entire area defines the uncertainty (statistical and systematic uncertainties combined).

## 6 Results

Figure 1 shows the distribution of the discriminant histograms, summed for bins with similar values of the  $s$ -channel minus  $t$ -channel signal contributions over the background expectation. We show the data, the  $s$ - and  $t$ -channel contributions as predicted by the SM and the different sources of background. Large negative values of the discriminant are dominated by the  $t$ -

channel contribution and large positive values are dominated by the  $s$ -channel contribution. The magnitude of the values of the discriminant for large negative values is greater than for large positive values, because we observe more  $t$ -channel events than  $s$ -channel events and the separation from background is better for  $t$ -channel events than for  $s$ -channel events.

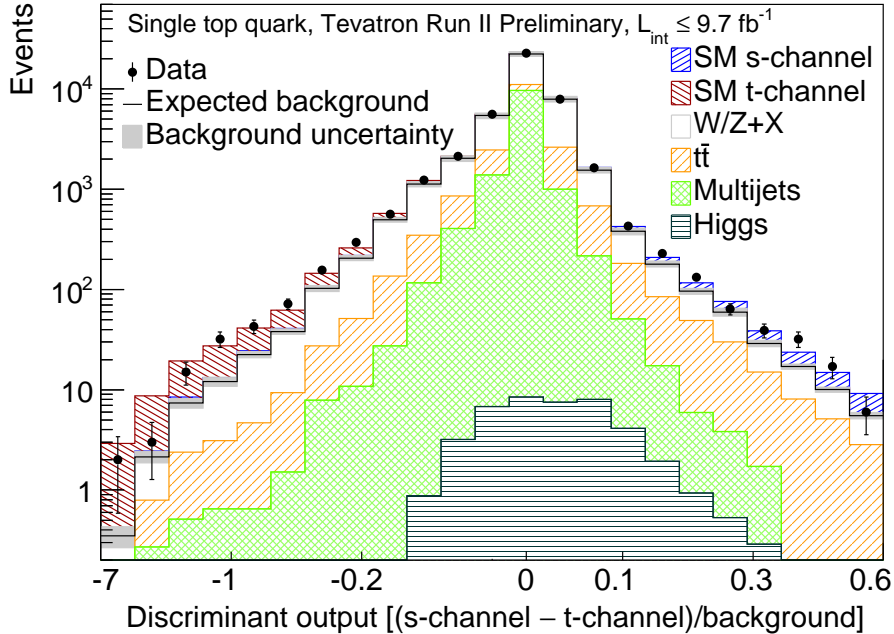


Figure 1: (Color online) Distribution of the discriminant, summed over bins with similar ratios of ( $s$ -channel  $-$   $t$ -channel) signals over background. Displayed are the data,  $s$ - and  $t$ -channel production as predicted in the SM and the expected background. The total expected background (black solid line) is shown with uncertainty (grey shaded band). A nonlinear scale is used on the abscissa to better display the range of values.

The extracted 2D posterior probability distribution as a function of  $\sigma_t$  and  $\sigma_s$  is presented in Fig. 2. The mean value and uncertainty in the individual cross sections are derived through the one-dimensional (1D) posterior probability functions, obtained by integrating the 2D posterior over the other variable. The most probable value for the combined  $t$ -channel cross section is  $\sigma_t = 2.25^{+0.29}_{-0.31}$  pb. The combined  $s + t$  cross section  $\sigma_{s+t}$  is measured without assuming the SM ratio of  $\sigma_s/\sigma_t$ , by forming a 2D posterior of  $\sigma_{s+t}$  versus  $\sigma_t$ , and then integrating over all possible values of  $\sigma_t$  to extract the 1D estimate of  $\sigma_{s+t}$ . The combined cross section is  $\sigma_{s+t} = 3.30^{+0.52}_{-0.40}$  pb ( $= 3.30^{+16\%}_{-12\%}$  pb). The total expected uncertainty on  $\sigma_{s+t}$  is 13%, and the expected uncertainty without considering systematic uncertainties is 8%. The systematic uncertainty on the measured cross section from the uncertainty on the top quark mass is negligible compared with the other uncertainties [16, 21]. Figure 3 shows the individual [20, 21] and combined (this note) measurements of the  $t$ - and  $s + t$ -channel cross sections including previous measurements of the individual [23, 21] and combined [25]  $s$ -channel cross sections.

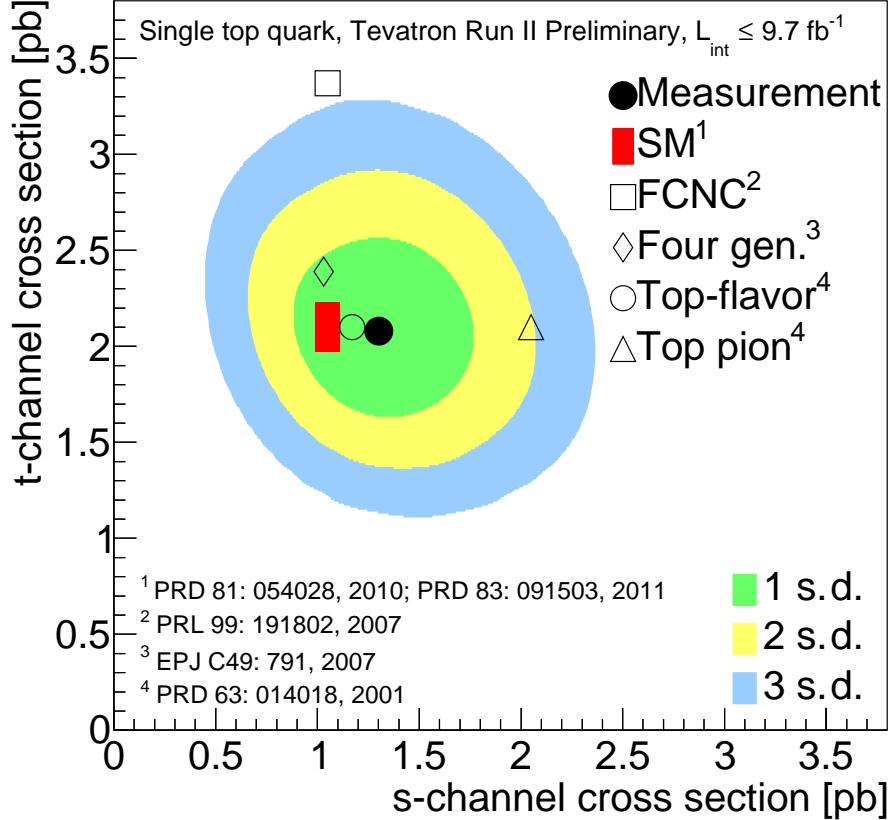


Figure 2: The 2D posterior probability with one, two, and three S.D. probability contours for the combination of the CDF and D0 analysis channels compared with the NLO+NNLL theoretical prediction of the SM [12, 9]. Several BSM predictions are shown, including four-quark generations with CKM matrix element  $|V_{ts}| = 0.2$  [51], a top-flavor model with new heavy bosons with  $m_x = 1 \text{ TeV}$  [6], a model of charged top-pions with  $m_{\pi^\pm} = 250 \text{ GeV}$  [6], and flavor changing neutral currents with an up-quark/top-quark/gluon coupling  $\kappa_u/\Lambda = 0.036$  [6, 52].

All measurements are consistent with the SM predictions.

The SM single-top-quark production cross section depends strongly on the square of the CKM matrix element  $|V_{tb}|$ , thus providing a way to measure  $|V_{tb}|$  directly without any assumption on the number of quark families or the unitarity of the CKM matrix [53]. However, sources of new physics beyond the SM could lead to a measured strength of the  $Wtb$  coupling  $|V_{tb}|$  different from 1. We extract  $|V_{tb}|$  assuming that top quarks decay predominantly to  $Wb$ .

We start with the same MVA discriminants for  $s$  and  $t$  channels as described before, and form a Bayesian posterior probability density for  $|V_{tb}|^2$  assuming a uniform prior probability distribution. Additional theoretical uncertainties are considered for the  $s$ - and  $t$ -channel cross sections [12, 9]. The extracted posterior probability distribution for  $|V_{tb}|^2$  is presented in Fig. 4.

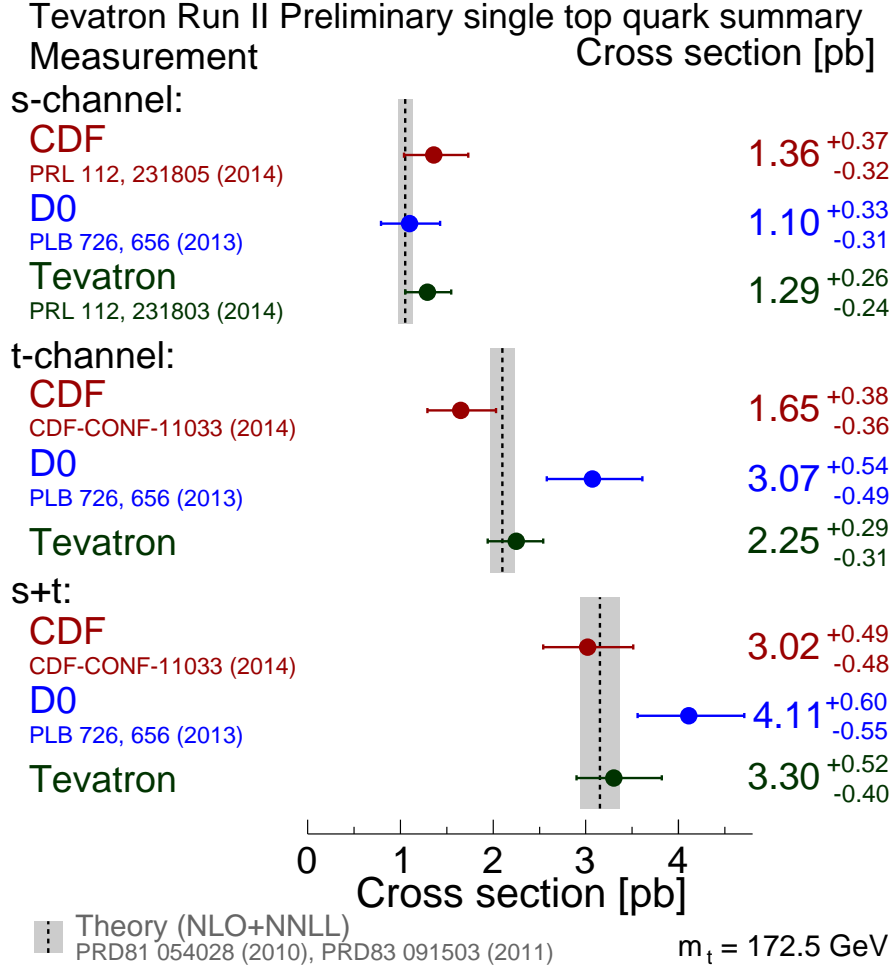


Figure 3: (Color online) Measured single-top-quark production cross sections from the CDF and D0 collaborations in different production channels, and the Tevatron combinations of these analyses compared with the NLO+NNLL theoretical prediction [12, 9].

We obtain  $|V_{tb}| = 1.02^{+0.06}_{-0.05}$ . If we restrict the prior to the SM region  $[0,1]$ , we extract a limit of  $|V_{tb}| > 0.92$  at 95% C.L.

## 7 Summary

In summary, for an integrated luminosity of up to  $9.7 \text{ fb}^{-1}$  per experiment, we report the final combination of single-top-quark production cross sections from CDF and D0 measurements assuming  $m_t = 172.5 \text{ GeV}$ . The cross section for  $t$ -channel production is found to be:

$$\sigma_t = 2.25^{+0.29}_{-0.31} \text{ pb.}$$

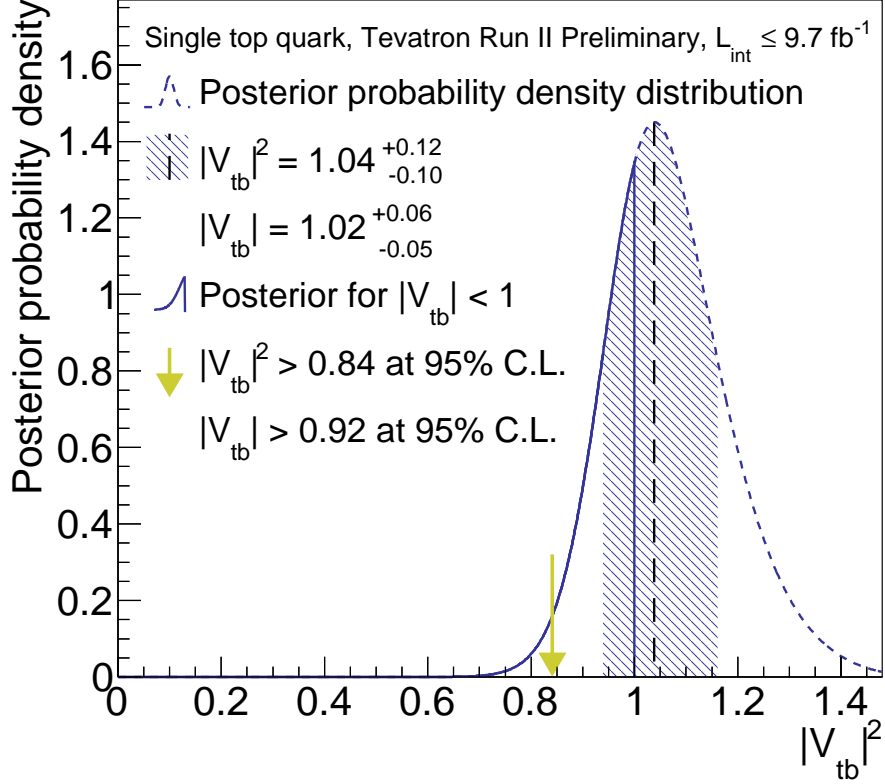


Figure 4: The posterior probability distribution for the combination of CDF and D0 analysis channels. The yellow region indicates the allowed values of  $|V_{tb}|^2$  corresponding to the limit of  $|V_{tb}| > 0.92$  at 95% C.L.

With no assumption on the relative  $s$ - and  $t$ -channel contributions, the total single-top-quark production cross section is:

$$\sigma_{s+t} = 3.30_{-0.40}^{+0.52} \text{ pb.}$$

Together with the combined  $s$ -channel cross section [25], this completes all single-top-quark cross-section measurements accessible at the Tevatron. All measurements are consistent with the SM predictions [12, 9]. Finally, we extract a direct limit on the CKM matrix element of  $|V_{tb}| > 0.92$  at 95% C.L., assuming a uniform prior within  $0 \leq |V_{tb}|^2 \leq 1$ .

## Acknowledgments

We thank the Fermilab staff and technical staffs of the participating institutions for their vital contributions. We acknowledge support from the DOE and NSF (USA), ARC (Australia), CNPq, FAPERJ, FAPESP and FUNDUNESP (Brazil), NSERC (Canada), NSC, CAS and CNSF (China), Colciencias (Colombia), MSMT and GACR (Czech Republic), the Academy of

Finland, CEA and CNRS/IN2P3 (France), BMBF and DFG (Germany), DAE and DST (India), SFI (Ireland), INFN (Italy), MEXT (Japan), the Korean World Class University Program and NRF (Korea), CONACyT (Mexico), FOM (Netherlands), MON, NRC KI and RFBR (Russia), the Slovak R&D Agency, the Ministerio de Ciencia e Innovación, and Programa Consolider-Ingenio 2010 (Spain), The Swedish Research Council (Sweden), SNSF (Switzerland), STFC and the Royal Society (United Kingdom), the A.P. Sloan Foundation (USA), and the EU community Marie Curie Fellowship contract 302103.

## References

- [1] C. E. Gerber and C. Vellidis, arXiv:1409.5038 [hep-ex].
- [2] T. A. Aaltonen *et al.* (CDF and D0 Collaborations), Phys. Rev. D **89** (2014) 072001.
- [3] N. Cabibbo, Phys. Rev. Lett. **10**, 531 (1963);  
M. Kobayashi and T. Maskawa, Prog. Theor. Phys. **49**, 652 (1973).
- [4] M. S. Chanowitz, Phys. Rev. D **79**, 113008 (2009).
- [5] J. Alwall, R. Frederix, J.-M. Gerard, A. Giammanco, M. Herquet, S. Kalinin, E. Kou, V. Lemaître, and F. Maltoni, Eur. Phys. J. C **49**, 791 (2007).
- [6] T. M. P. Tait and C. P. Yuan, Phys. Rev. D **63**, 014018 (2000).
- [7] S. S. D. Willenbrock and D. A. Dicus, Phys. Rev. D **34**, 155 (1986).
- [8] C.-P. Yuan, Phys. Rev. D **41**, 42 (1990).
- [9] N. Kidonakis, Phys. Rev. D **83**, 091503 (2011).
- [10] S. Cortese and R. Petronzio, Phys. Lett. B **253**, 494 (1991).
- [11] T. M. P. Tait, Phys. Rev. D **61**, 034001 (2000).
- [12] N. Kidonakis, Phys. Rev. D **81**, 054028 (2010).
- [13] K. A. Olive *et al.* (Particle Data Group), Chin. Phys. C **38**, 090001 (2014).
- [14] T. Aaltonen *et al.* (CDF Collaboration), Phys. Rev. Lett. **103**, 092002 (2009).
- [15] T. Aaltonen *et al.* (CDF Collaboration), Phys. Rev. D **81** (2010) 072003.
- [16] T. Aaltonen *et al.* (CDF Collaboration), Phys. Rev. D **82**, 112005 (2010).
- [17] V. M. Abazov *et al.* (D0 Collaboration), Phys. Rev. Lett. **103**, 092001 (2009).
- [18] V. M. Abazov *et al.* (D0 Collaboration), Phys. Rev. D **84**, 112001 (2011).

- [19] T. A. Aaltonen *et al.* (CDF Collaboration), arXiv:1407.4031 [hep-ex].
- [20] CDF Collaboration, CDF-CONF-11033 (2014).
- [21] V. M. Abazov *et al.* (D0 Collaboration), Phys. Lett. B **726**, 656 (2013).
- [22] V. M. Abazov *et al.* (D0 Collaboration), Phys. Lett. B **705**, 313 (2011).
- [23] T. A. Aaltonen *et al.* (CDF Collaboration), Phys. Rev. Lett. **112**, 231804 (2014).
- [24] T. A. Aaltonen *et al.* (CDF Collaboration), Phys. Rev. Lett. **112**, 231805 (2014).
- [25] T. A. Aaltonen *et al.* (CDF and D0 Collaborations), Phys. Rev. Lett. **112**, 231803 (2014).
- [26] G. Aad *et al.* (ATLAS Collaboration), Phys. Lett. B **717**, 330 (2012).
- [27] G. Aad *et al.* (ATLAS Collaboration), arXiv:1406.7844 [hep-ex].
- [28] S. Chatrchyan *et al.* (CMS Collaboration), J. High Energy Phys. 12 (2012) 035.
- [29] V. Khachatryan *et al.* (CMS Collaboration), J. High Energy Phys. 1406 (2014) 090.
- [30] G. Aad *et al.* (ATLAS Collaboration), Phys. Lett. B **716** 142 (2012).
- [31] S. Chatrchyan *et al.* (CMS Collaboration), Phys. Rev. Lett. **112**, 231802 (2014).
- [32] D. Acosta *et al.* (CDF Collaboration), Phys. Rev. D **71**, 032001 (2005).
- [33] V. M. Abazov *et al.* (D0 Collaboration), Nucl. Instrum. Meth. A **565**, 463 (2006).
- [34] J. Freeman, T. Junk, M. Kirby, Y. Oksuzian, T. Phillips, F. Snider, M. Trovato, J. Vizan, and W. Yao, Nucl. Instrum. Methods A **697**, 64 (2013).
- [35] V. M. Abazov *et al.* (D0 Collaboration), Nucl. Instrum. Methods A **620**, 490 (2010);  
V. M. Abazov *et al.* (D0 Collaboration), Nucl. Instrum. Methods A **763**, 290 (2014);
- [36] S. Alioli, P. Nason, C. Oleari, and E. Re, J. High Energy Phys. 09 (2009) 111.
- [37] E. E. Boos, V. E. Bunichev, L. V. Dudko, V. I. Savrin, and V. V. Sherstnev, Phys. Atom. Nucl. **69**, 1317 (2006). We use SINGLETOP version 4.2p1.
- [38] Z. Sullivan, Phys. Rev. D **70**, 114012 (2004).
- [39] J. M. Campbell, R. Frederix, F. Maltoni, and F. Tramontano, Phys. Rev. Lett. **102**, 182003 (2009).
- [40] M. L. Mangano, M. Moretti, F. Piccinini, R. Pittau, and A.D. Polosa, J. High Energy Phys. 07 (2003) 001. We use ALPGEN version 2.11.
- [41] T. Sjöstrand, S. Mrenna, and P. Skands, J. High Energy Phys. 05 (2006) 026. We use PYTHIA version 6.409.

- [42] The ATLAS and CDF and CMS and D0 Collaborations, arXiv:1403.4427 [hep-ex].
- [43] G. Aad *et al.* (ATLAS Collaboration), Phys. Rev. D **90**, 052004 (2014).
- [44] V. Khachatryan *et al.* (CMS Collaboration), arXiv:1407.0558 [hep-ex].
- [45] S. Chatrchyan *et al.* (CMS Collaboration), Phys. Rev. D **89**, 092007 (2014); G. Aad *et al.* (ATLAS Collaboration), Phys. Lett. B **716**, 1 (2012).
- [46] R. Brun and F. Carminati, CERN Program Library Long Writeup, Report No. W5013, 1993.
- [47] S. Moch and P. Uwer, Phys. Rev. D **78**, 034003 (2008). The top-quark-pair cross section is  $7.46 \pm 0.75$  pb ( $m_t = 172.5$  GeV).
- [48] R. K. Ellis, Nucl. Phys. Proc. Suppl. **160**, 170 (2006). We use MCFM version 5.1.
- [49] J. Baglio and A. Djouadi, J. High Energy Phys. 10 (2010) 064.
- [50] I. Bertram *et al.*, FERMILAB-TM-2104 (2000).
- [51] J. Alwall *et al.*, Eur. Phys. J. C **49**, 791 (2007).
- [52] V. M. Abazov *et al.* (D0 Collaboration), Phys. Rev. Lett. **99**, 191802 (2007).
- [53] V. M. Abazov *et al.* (D0 Collaboration), Phys. Rev. D **78**, 012005 (2008).